Published OnlineFirst July 20, 2021; DOI: 10.1158/1078-0432.CCR-21-1204

A Phase I Dose-Escalation and Expansion Study of Telaglenastat in Patients with Advanced or Metastatic Solid Tumors

James J. Harding[1], Melinda Telli[2], Pamela Munster[3], Martin H. Voss[1], Jeffrey R. Infante[4], Angela DeMichele[5], Mark Dunphy[1], Mai H. Le[6], Chris Molineaux[6], Keith Orford[6], Frank Parlati[6], Sam H. Whiting[6], Mark K. Bennett[6], Nizar M. Tannir[7], and Funda Meric-Bernstam[7]

ABSTRACT

Purpose: Glutamine is a critical fuel for solid tumors. Interference with glutamine metabolism is deleterious to neoplasia in preclinical models. A phase I study of the oral, first-in-class, glutaminase (GLS) inhibitor telaglenastat was conducted in treatment-refractory solid tumor patients to define recommended phase II dose (RP2D) and evaluate safety, pharmacokinetics (PK), pharmacodynamics (PD), and antitumor activity.

Patients and Methods: Dose escalation by 3 + 3 design was followed by exploratory tumor-/biomarker-specific cohorts.

Results: Among 120 patients, fatigue (23%) and nausea (19%) were the most common toxicity. Maximum tolerated dose was not reached. Correlative analysis indicated >90% GLS inhibition in platelets at plasma exposures >300 nmol/L, >75% tumoral GLS inhibition, and significant increase in circulating glutamine. RP2D was defined at 800 mg twice-daily. Disease control rate (DCR) was 43% across expansion cohorts (overall response rate 5%, DCR 50% in renal cell carcinoma).

Conclusions: Telaglenastat is safe, with a favorable PK/PD profile and signal of antitumor activity, supporting further clinical development.

Introduction

Many tumors consume the amino acid glutamine to meet demands of rapid cell growth (1). The first step in glutamine metabolism is catalyzed by the enzyme glutaminase (GLS), which converts glutamine to glutamate. Glutamate fuels the tricarboxylic acid cycle (TCA) cycle for ATP production, biosynthetic intermediates synthesis (e.g., amino acids, fatty acids, nucleotides), and glutathione production to balance cellular oxidative stress (2, 3). Several tumor histologies have pronounced GLS upregulation, including renal cell carcinoma (RCC), triple-negative breast cancer (TNBC), non–small cell lung cancer (NSCLC), and mesothelioma (4). Cell lines derived from these tumor types are sensitive to glutamine withdrawal or GLS inhibition, making GLS an appealing target for therapeutic intervention in multiple solid tumor histologies (5–11).

Specific genomic alterations contribute to glutamine dependency in solid tumors. Von Hippel-Lindau (VHL) loss-of-function mutations, found primarily in clear cell RCC, upregulate glutamine metabolism and glutamine utilization to fuel production of TCA cycle intermediates, lipids, and nucleotides (12, 13). *KRAS* and *MYC* alterations are associated with metabolic reprogramming that elevates glutamine-dependent biosynthetic pathways to maintain redox balance and support tumor growth (9, 14–19). Mutations in TCA cycle enzymes, fumarate hydrogenase (FH), succinate dehydrogenase (SDH), and isocitrate dehydrogenase (IDH), lead to accumulation of fumarate, succinate, and 2-hydroglutaric acid, respectively. These metabolites inhibit α-ketoglutarate–using enzymes, causing malignant transformation (20). Tumors bearing these mutations become more dependent on glutamine-derived glutamate for TCA cycle anaplerosis (21, 22).

Despite the known role of glutamine in tumor metabolism and the abundance of preclinical data demonstrating tumor sensitivity to reduced glutamine, either through withdrawal from growth medium, GLS knockdown, or inhibition of GLS (5–11), testing these preclinical findings in the clinic has been highly problematic. Several classes of compounds that target non-selectively glutamine metabolism have been examined, but all have been limited by toxicity or poor pharmacokinetic (PK) properties—thus the operating characteristics of targeting glutamine in patients with solid tumors remain unclear (2).

Telaglenastat (CB-839) is an investigational, first-in-class, small molecule, oral allosteric and selective inhibitor of GLS. In preclinical studies, telaglenastat exhibits both cytostatic and cytotoxic antiproliferative activity across several tumor cell lines (23–25) and has cytostatic-suppressive effects against tumor growth in a number of different solid tumor xenograft mouse models (e.g., RCC, NSCLC, TNBC, hematologic malignancies), both alone and in combination

[1]Memorial Sloan Kettering Cancer Center and Weill Medical College, New York, New York. [2]Stanford University School of Medicine, Stanford, California. [3]University of California at San Francisco, San Francisco, California. [4]Sarah Canon Research Institute, Tennessee Oncology PLLC, Nashville, Tennessee. [5]University of Pennsylvania, Philadelphia, Pennsylvania. [6]Calithera Biosciences, Inc., South San Francisco, California. [7]The University of Texas MD Anderson Cancer Center, Houston, Texas.

Note: Supplementary data for this article are available at Clinical Cancer Research Online (http://clincancerres.aacrjournals.org/).

Current address for J.R. Infante: Department of Oncology, Janssen, Raritan, NJ.

Prior Presentation: Presented in part at the AACR-NCI-EORTC 27th International Symposium in Molecular Targets and Cancer Therapeutics, Boston, MA, November 5–9, 2015, and American Society of Clinical Oncology Annual Meeting, Chicago, IL, May 29-June 2, 2015.

Corresponding Author: James J. Harding, Memorial Sloan Kettering Cancer Center, 300 East 66th Street, New York, NY. Phone: 646-888-4314; Fax: 646-888-4255; E-mail: hardinj1@mskcc.org

Clin Cancer Res 2021;27:4994–5003

doi: 10.1158/1078-0432.CCR-21-1204

Published OnlineFirst July 20, 2021; DOI: 10.1158/1078-0432.CCR-21-1204

Translational Relevance

Dependency of tumors on glutamine may be targeted by inhibition of glutaminase (GLS), an enzyme that catalyzes the first dedicated step in glutamine metabolism. This phase I study of the novel GLS inhibitor telaglenastat demonstrated safety, robust GLS inhibition with favorable PK, and signal of antitumor activity.

with other anticancer therapies (4, 23–30). Anticancer effects are also observed with telaglenastat or GLS knockdown in preclinical tumor models that harbor mutations in *KRAS, MYC*, and TCA enzymes, providing the rationale for clinical evaluation in mutational-specific context (9, 18, 22, 31). Therefore, strong rationale exists for a phase I study of telaglenastat for treatment of solid tumors with predicted sensitivity based on mutational metabolic reprogramming.

Patients and Methods

Study design

This first-in-human, open-label, phase I trial (NCT02071862) included dose escalation and dose expansion of telaglenastat as a single agent in patients with advanced and/or treatment-refractory solid tumors (Supplementary Fig. S1). The primary objective was to determine safety, tolerability, and recommended phase II dose (RP2D). Secondary objectives included PK, pharmacodynamics, and antitumor activity. Patients were enrolled according to a traditional 3+3 design in dose escalation. Tumor-specific expansions in solid tumor histologies or histology-agnostic, genomically driven cohorts of interest were then opened to further define safety and explore efficacy. The study was conducted in accordance with the ethics principles of the Declaration of Helsinki and the International Council of Harmonization Guidelines on Good Clinical Practice. All patients provided written informed consent.

Patient selection

Eligible patients had to be ≥18 years of age, ECOG performance status 0–1, measurable disease per RECIST v1.1 criteria (32), adequate organ function, with histologically confirmed diagnosis of locally advanced, inoperable, metastatic, and/or treatment-refractory solid tumors for which no therapies that confer clinical benefit were available. For genomically selected cohorts (*KRAS*-mutated NSCLC, *IDH1/2*-mutated tumors, *SDH*-deficient tumors, *FH*-deficient tumors, *MYC*-amplified tumors), oncogenic driver mutations were identified by local standard-of-care genomic testing. *MYC* amplifications had to be ≥5-fold amplified by the local method. Patients were excluded if receiving concomitant anticancer therapy had untreated/active brain metastases or CNS disease, or had a severe medical illness that would interfere with study participation (see Supplementary Data for details).

Study treatment

Telaglenastat was administered orally in 21-day cycles until disease progression or intolerable toxicity. Initial dose-escalations levels were 100, 150, 250, 400, 600, and 800 mg for the 3 times daily (TID) "fasted" cohort (8 hours without food for morning dose, on empty stomach for midday and evening doses). Starting dose was based on preclinical toxicology studies and PK modeling that suggested that sustained plasma exposures of telaglenastat over 200 ng/mL would maximize target inhibition (Calithera, data on file). During the conduct of the study, increased exposure of telaglenastat was observed when dosed with food, and twice daily (BID) dosing with food ("BID-fed") was explored with 3 dose-escalating cohorts: 600, 800, and 1,000 mg BID. Starting dose in the BID-fed cohorts was based on the highest previously cleared dose level in TID escalation cohort. Intrapatient dose escalation was permitted after completion of cycle 1 once the next higher dose level had been demonstrated to be well tolerated. For dose expansion, patients received either 600 or 800 mg per oral route (PO) BID.

Safety and efficacy evaluations

All patients were evaluated with medical history, physical examinations, and clinical laboratory results weekly for the first cycle, then on day 1 of each subsequent cycle. Adverse events (AE) were recorded by Common Toxicity Criteria for Adverse Events (CTCAE) v.4 from first dose of study drug up to 28 days after the last dose. Disease assessments with CT scans or MRI were performed at baseline and on day 1 of every third cycle (every 9 weeks). Tumor-response assessments were completed by RECIST v 1.1 criteria (32) for all solid tumors except pleural mesothelioma that used the modified RECIST criteria (33).

Pharmacokinetics

PK samples were collected on days 1 and 15 of cycle 1 at the following times: Predose, 0.5, 1, 2, 4, 6, and 8 hours postdose. Plasma concentrations of telaglenastat and glutamine were determined using HPLC/MS/MS. Telaglenastat PK parameters were estimated by noncompartmental analysis method. C_{max} and T_{max} were determined directly from the observed data, and AUC was calculated for days 1 and 15 of cycle 1.

Pharmacodynamics

GLS inhibition was measured in circulating platelets. Platelets were sampled predose and 4 hours after dosing on cycle 1, day 1. Paired fresh tumor samples were also assessed by similar methodology in patients who underwent optional pretreatment and on-treatment biopsies (cycle 2 and day 1). Platelet pellets from −80°C freezer were thawed on ice and resuspended in 230 μL of ice-cold lysis buffer. Samples were subjected to two rounds of homogenization on a Bioruptor for 5 minutes per cycle and filtered over a gel-filtration spin column (Zeba Spin Desalting Column, 7K MWCO). Spin columns were centrifuged at 2,500 RPM, 4–5 minutes, 4°C. Spin-filtered samples were serially diluted in a 384-well microplate for assay. Homogenates were quantified for total protein amount (BCA protein assay). Enzymatic assays were assembled in low-volume black 384-well HE microplates (Molecular Devices) by mixing (i) 5 μL platelet or tissue homogenates, (ii) 5 μL glutamate dehydrogenase (GDH), and (iii) 5 μL substrate ($NADP^+$ and glutamine). Each component was separately prepared as a 3× solution and kept at room temperature. A 3×-GDH-containing solution was prepared by diluting GDH into assay buffer to reach a final concentration of 18 U/mL GDH. A 3×-substrate-containing solution was prepared by diluting glutamine and $NADP^+$ stock solutions into assay buffer to reach final concentrations of 30 and 6 mmol/L, respectively. Fully assembled reactions were thus 15 μL in volume and contained 6 U/mL GDH, 10 mmol/L glutamine, 2 mmol/L $NADP^+$, and various amounts of platelet or tissue homogenate. A second sample of each serial dilution was incubated without glutamine added. Generation of NADPH was monitored by fluorescence (Ex340/Em460 nm) every minute for 15 minutes on a SpectraMax M5e plate reader (Molecular Devices at 25°C). Relative fluorescence units (RFU) were converted to units of NADPH concentration (μmol/L) using a standard curve of NADPH. Under these assay conditions, up to

Published OnlineFirst July 20, 2021; DOI: 10.1158/1078-0432.CCR-21-1204

75 μmol/L glutamate is stoichiometrically converted to α-ketoglutarate/NADPH by GDH.

For the on-treatment biopsies, the GLS assay was specifically developed to take advantage of the slow dissociation between telaglenastat and GLS when cell/tissue lysates are prepared in the presence of high salt and low phosphate concentrations, keeping the enzyme in an inhibited state; inhibited GLS activity was then measured by separating the enzyme–inhibitor complex from free substrate and inhibitor and determining the activity of the residual uninhibited enzyme.

RP2D determination and DLT definition

Dose escalation followed a standard 3+3 design with a minimum of 3 patients assigned per dose level. If 0 of 3 or 1 of 6 patients in a cohort experienced a dose-limiting toxicity (DLT), dose escalation would continue to enroll per protocol. MTD was defined as the highest dose level with either no DLTs reported in 3 DLT-evaluable patients, or ≤1 DLT in 6 DLT-evaluable patients. MTD was exceeded if >1 of 3 or ≥2 of 6 patients experienced a DLT.

DLTs were evaluated only in patients receiving at least 75% of planned doses in the first treatment cycle and defined as any AE that could not be determined to be unrelated to study treatment, occurs within the first treatment cycle, and meets at least one of the following criteria: (i) Any grade ≥3 clinically significant non-hematologic toxicity per the CTCAE v.4, except nausea/vomiting/diarrhea lasting <48 hours and controlled with antiemetic/antidiarrheal therapy, grade 3 hyperglycemia lasting <72 hours with standard antidiabetic therapy, laboratory abnormalities reversible to grade ≤1 or baseline status within 72 hours with outpatient care and/or monitoring, or that are considered not clinically significant by the investigator; (ii) grade 4 neutropenia (ANC $< 0.5 \times 10^9$/mL); (iii) grade 3 febrile neutropenia (ANC $< 1.0 \times 10^9$/L with temperature ≥38.3°C); (iv) grade 4 thrombocytopenia (platelet count $< 25.0 \times 10^9$/L) lasting >4 days or requiring platelet transfusion; (v) grade ≥3 thrombocytopenia (platelet count $<50.0 \times 10^9$/L) associated with grade ≥3 bleeding; (vi) any other AE that is felt to be treatment-limiting in the medical opinion of the principal investigator and medical monitor. After each cohort was cleared for safety, an additional 4 patients with biopsy-amenable disease for mandatory pre- and on-treatment biopsies could be enrolled.

Per protocol, RP2D was to be selected based on MTD or, if MTD was not reached, other considerations, including: (i) Proportionality of dose-exposure relationship; (ii) magnitude of systemic GLS inhibition in platelets (goal: ≥90% inhibition at C_{min}); and (iii) overall safety/efficacy observations, including concurrent clinical trials.

Statistical analysis

Descriptive statistics were used to analyze the data, and summary statistics for continuous variables. Categorical variables are presented as frequency counts and percentages. All patients who received at least one telaglenastat dose were analyzed for safety. Results were tabulated by frequency, organ systems affected, and relationship to study treatment.

Using a Simon 2-Stage design, the sample size of 11 patients per expansion cohort was selected to allow adequate confirmation of safety and tolerability of telaglenastat and to identify evidence of preliminary clinical activity worthy of further investigation. In cases of clinical activity in any of the expansion cohorts based on response rate (i.e., at least 1 responder from the initial 11 patients), the protocol allowed an additional 26 patients for a total of 37 patients per cohort. With this design, the null hypothesis was an objective response rate (ORR) of ≤2% versus the alternate hypotheses of an ORR ≥15%, which would be reasonable for treatment-refractory solid tumors. A sample size of 37 patients per tumor type cohort would maintain an alpha level of 0.05 and 0.80 power. ORR was defined as the proportion of patients with complete response (CR) or partial response (PR) and calculated with a 95% confidence interval. Disease control rate (DCR) was defined as overall response rate + stable disease. The efficacy analysis set comprised all patients who completed 1 post-baseline tumor assessment. Patients who discontinued study medication early due to treatment-related toxicity or due to disease-related death or symptomatic deterioration (clinical progression) must have had received at least 48 doses TID or 32 doses BID to be considered evaluable for efficacy.

Results

Patients

From February 2014 to October 2016, 56 patients (32 TID-fasted; 24 BID-fed) enrolled in dose-escalation and 64 in dose-expansion parts of the trial (**Table 1**). In dose escalation, 20 patients (36%) had TNBC, 9 (16%) RCC, 5 (9%) NSCLC, 5 (9%) mesothelioma, and the remaining with cancers of the bone, liver, colorectal, soft tissue, stomach, uterus, and gall bladder. In dose expansion, 22 patients enrolled in the RCC cohort, 9 NSCLC, 7 TNBC, 1 mesothelioma, and the remaining 25 across the 5 mutation-specific cohorts. Median age of patients was 60 and 59.5 years for dose escalation and dose expansion, respectively. Patients were heavily pretreated; >50% received ≥4 prior lines of systemic therapy (combined adjuvant/metastatic). High levels of GLS, based on H-score, were seen with immunohistochemical staining of archival tumor samples ($n = 36$) from patients with TNBC, NSCLC, RCC, mesothelioma, and SDH-deficient GIST (Supplementary Fig. S2). H-score was >100 for all but two patients (1 TNBC, H-score = 0; 1 TCA cycle mutant, H-score = 10).

Safety

Of 56 patients treated in dose escalation, 3 DLTs occurred in 2 patients in the TID-fasted cohort: 1 had creatinine increase at the 250 mg TID dose; 1 had alanine transaminase (ALT) increase and aspartate transaminase (AST) increase at 400 mg TID. No DLTs occurred on the BID-fed schedule. MTD was therefore not established.

Overall, across doses and schedules, treatment-related AEs of any grade were reported in 87/120 (72.5%) patients (**Table 2**): Fatigue (23%), nausea (19%), ALT increased (17%), AST increased (13%), and photophobia (11%). Patients receiving telaglenastat BID-fed had a lower incidence of treatment-related grade 3/4 AEs than those on the TID-fasted schedule [3/88 (3%) BID-fed vs. 7/32 (22%) TID-fasted]. In particular, grade 3/4 AST or ALT increase was significantly less frequent on the BID-fed schedule (1% AST, 2% ALT) than the TID-fasted schedule (16% ALT, 16% AST). Concurrent bilirubin elevation with AST/ALT elevation was rare; no patients on either schedule met criteria for the Hy's Law. There were no grade 5 AEs. Overall, 50 of 120 patients (42%) had dose interruptions, primarily due to AEs, 17 (14%) had dose reductions, and 4 (3%) had dose increased.

Serious AEs (SAE) occurred in 27 (22.5%) patients in dose-escalation and -expansion cohorts, most of which were considered unrelated to treatment. Four treatment-related SAEs occurred in 3 patients: ALT and AST increase (1 patient, 400 mg TID), blood creatinine increase (250 mg TID), and a grade 2 convulsion deemed possibly related to treatment (1,000 mg BID), which occurred after the first dose in a patient with metastatic TNBC who had 3 previously undiagnosed MRI-documented brain metastases. Seven

Published OnlineFirst July 20, 2021; DOI: 10.1158/1078-0432.CCR-21-1204

Table 1. Demographics and baseline characteristics.

	Telaglenastat dose-escalation			Telaglenastat dose-expansion
	TID-Fasted (*N* = 32)	BID-Fed (*N* = 24)	Total (*N* = 56)	(*N* = 64)
Median age, y (range)	59.0 (33.0–78.0)	62.5 (36.0–88.0)	60.0 (33.0–88.0)	59.5 (19.0–93.0)
Female, *n* (%)	23 (71.9)	13 (54.2)	36 (64.3)	38 (59.4)
Race, *n* (%)				
White	22 (68.8)	21 (87.5)	43 (76.8)	49 (76.6)
Black or African American	4 (12.5)	3 (12.5)	7 (12.5)	7 (10.9)
Other	6 (18.8)	0	6 (10.7)	8 (12.5)
ECOG performance status, *n* (%)				
0	8 (25.0)	6 (25.0)	14 (25.0)	16 (25.0)
1	24 (75.0)	18 (75.0)	42 (75.0)	48 (75.0)
Diagnosis, *n* (%)				
Renal cell carcinoma	4 (12.5)	5 (20.8)	9 (16.1)	25 (39.1)
Non–small cell lung cancer	4 (12.5)	1 (4.2)	5 (8.9)	9 (14.1)[a]
Triple-negative breast cancer	11 (34.4)	9 (37.5)	20 (35.7)	7 (10.9)
Mesothelioma	3 (9.4)	2 (8.3)	5 (8.9)	1 (1.6)
Other	10 (31.2)	7 (29.2)	17 (30.4)	22 (34.4)
Known TCA cycle mutations				
IDH mutation	0	4 (16.7)	4 (7.1)	10 (15.6)
SDH-deficient GIST	1 (3.1)	2 (8.4)	3 (5.4)	3 (4.7)
SDH-deficient non-GIST	0	0	0	3 (4.7)
FH-deficient	0	0	0	4 (6.3)
c-MYC amplification	0	0	0	5 (9.4)
Median time since locally advanced/metastatic disease (mo; range)	24.4 (3.5–124.4)	24.1 (2.0–176.6)	24.4 (2.0–176.6)	26.0 (1.3–354.5)
Prior treatments				
≥1 Prior surgery	29 (90.6)	21 (87.5)	50 (89.3)	49 (76.6)
≥1 Prior radiotherapy	13 (40.6)	11 (45.8)	24 (42.9)	28 (43.8)
Prior systemic therapies				
<2	2 (6.3)	6 (25.0)	8 (14.3)	11 (17.2)
2 to 3	8 (25.0)	4 (16.7)	12 (21.4)	24 (37.5)
≥4	22 (68.8)	14 (58.3)	36 (64.3)	29 (45.3)

Abbreviations: BID, twice daily; ECOG, Eastern Cooperative Oncology Group; *FH*, fumarate hydrogenase; GIST, gastrointestinal stromal tumor; *IDH*, isocitrate dehydrogenase; *SDH*, succinate dehydrogenase; TID, three times daily.
[a]*KRAS*-mutated.

patients died during the study-reporting period, all due to progressive disease (PD).

Pharmacokinetics

Following multiple administrations of 100 to 800 mg telaglenastat under fasted conditions, median t_{max} ranged from 1.0 to 2.0 hours over the dose range (**Table 3**). For the 100, 150, 250, 400, 600, and 800 mg TID dose levels, mean AUC_{last} were 2,150, 7,603, 4,626, 3,850, 5,162, and 5,832 ng·h/mL, respectively. Mean C_{max} values for the same dose levels were 395, 1,444, 914, 818, 1,142, and 1,058, respectively. Because blood samples were collected only for the first 8 hours before subsequent treatment with telaglenastat, the terminal phase could not be characterized for most patients, except one each in the 250 and 600 mg dose levels (3.73 hours). On the TID schedule, patients received telaglenastat without food throughout dosing, with the exception of cycle 2, day 1, when telaglenastat was administered with food. AUC_{0-8h} and C_{max} values were approximately 1.5-fold higher under fed conditions when compared with fasted conditions (**Table 3**). The average t_{max} with food was delayed by 2–3 hours compared with fasted conditions. On the basis of these observations, telaglenastat was administered on a BID schedule with food in all subsequent treatment cohorts.

Under PK evaluation under the BID-fed schedule showed that after approximately 2 weeks of dosing (cycle 1, day 15), median t_{max} ranged from 4.0 to 6.0 hours, suggesting a delayed absorption due to food effect. Exposure appeared to increase from 600 ($n = 41$) to 800 mg ($n = 10$), with mean AUC_{0-8h} of 7,611 and 9,660 ng*h/mL, respectively, and C_{max} of 1,455 and 1,774, respectively. For patients receiving 1,000 mg BID-fed ($n = 4$), mean AUC_{0-8}, AUC_{0-8h}, C_{max}, and median C_{min} were 915 ng·h/mL, 5,073 ng·h/mL, 5,005 ng/mL, and 147 ng/mL, respectively. Mean t_{max} for the 600, 800, and 1,000 mg BID-fed groups was 4.00, 4.00, and 6.08 hours, respectively (**Table 3**).

To further evaluate the effect of food on telaglenastat exposure, PK parameters were determined after the first administration of telaglenastat on cycle 1, day 1 under both fasted and fed regimens. Patients receiving 600 mg BID with food experienced a >3-fold increase in mean AUC_{0-8h} and C_{max}, compared with those receiving 600 mg BID while fasted. At the 800 mg BID dose, AUC_{0-8h} and C_{max} was 1.3-fold higher with fed than fasted dosing. Because of the associated delay in t_{max} and the flattening of the PK curve, these data supported the switch from TID dosing without food to BID dosing with food (Supplementary Fig. S3; Supplementary Table S1).

Pharmacodynamics

Measurement of GLS activity in peripheral platelets demonstrated >90% inhibition of GLS activity at plasma telaglenastat exposures >250 ng/mL (**Fig. 1A**). In patients with paired biopsies ($n = 5$) tumor GLS was inhibited by at least 75% (Cycle 2, Day 1), with exception

Published OnlineFirst July 20, 2021; DOI: 10.1158/1078-0432.CCR-21-1204

Table 2. Treatment-related AEs by preferred term in ≥5% of patients.

	Single-agent telaglenastat, TID-fasted ($n = 32$)			Single-agent telaglenastat, BID-fed ($n = 88$)		
Preferred term, *n* (%)	**All grades**	**Grade 3**	**Grade 4**	**All grades**	**Grade 3**	**Grade 4**
Patients with ≥1 treatment-emergent AE	30 (93.8)	9 (28.1)	3 (9.4)	84 (95.5)	28 (31.8)	5 (5.7)
Patients with ≥1 treatment-related AE	23 (71.9)	4 (12.5)	3 (9.4)	64 (72.7)	3 (3.4)	0
Related AEs						
Fatigue	7 (21.9)	0	0	21 (23.9)	0	0
Nausea	2 (6.3)	0	0	21 (23.9)	0	0
Alanine aminotransferase increased	6 (18.8)	5 (15.6)	0	14 (15.9)	2 (2.3)	0
Aspartate aminotransferase increased	6 (18.8)	3 (9.4)	2 (6.3)	10 (11.4)	1 (1.1)	0
Photophobia	1 (3.1)	0	0	12 (13.6)	0	0
Vomiting	4 (12.5)	0	0	5 (5.7)	0	0
Blood alkaline phosphatase increased	2 (6.3)	1 (3.1)	0	6 (6.8)	1 (1.1)	0
Decreased appetite	0	0	0	8 (9.1)	0	0
γ-Glutamyltransferase increased	1 (3.1)	0	1 (3.1)	7 (8.0)	2 (2.3)	0
Anemia	0	0	0	5 (5.7)	1 (1.1)	0
Blood creatinine increased	1 (3.1)	1 (3.1)	0	4 (4.5)	0	0
Constipation	2 (6.3)	0	0	3 (3.4)	0	0
Hypomagnesemia	0	0	0	4 (4.5)	0	0
Thrombocytopenia	0	0	0	4 (4.5)	0	0
Blood bilirubin increased	0	0	0	3 (3.4)	0	0
Diarrhea	1 (3.1)	0	0	2 (2.3)	0	0
Dysgeusia	1 (3.1)	0	0	2 (2.3)	0	0
Neuropathy peripheral	1 (3.1)	0	0	2 (2.3)	0	0
Photopsia	1 (3.1)	0	0	2 (2.3)	0	0
Vision blurred	0	0	0	3 (3.4)	0	0
Weight decreased	0	0	0	3 (3.4)	0	0
Abdominal distension	0	0	0	2 (2.3)	0	0
Activated partial thromboplastin time prolonged	0	0	0	2 (2.3)	0	0
Ammonia increased	0	0	0	2 (2.3)	0	0
Dyspepsia	0	0	0	2 (2.3)	0	0
Gastroesophageal reflux disease	0	0	0	2 (2.3)	0	0
Hyponatremia	0	0	0	2 (2.3)	0	0

Note: No grade 5 AEs.
Abbreviations: AE, adverse event; BID, twice daily; TID, three times daily.

of 1 patient who had low systemic exposure, likely due to radical gastrectomy (**Fig. 1B**). Plasma glutamine increased by approximately 150% on cycle 1, day 15 relative to predose on cycle 1, day 1 ($P = 0.0073$; $n = 6$; **Fig. 1C**).

RP2D selection

The initial dose selected for dose expansion was 600 mg BID based on available safety and PK data. Over the course of study, emerging PK/PD data demonstrated greater GLS inhibition with higher exposure at the 800-mg dose. In addition, the 800 mg dose led to higher exposure with equivalent safety. Thus, the final RP2D that was selected was 800 mg BID with food. Because RP2D was not selected until after initiation of the dose expansion phase, more patients received 600 mg BID ($n = 55$) than the final RP2D of 800 mg BID ($n = 11$).

Clinical activity

Of 101 patients evaluable for efficacy, 27 were in TID dose escalation, 16 in BID dose escalation, and 58 in the expansion cohorts (BID dosing); 4, 8, and 3 patients, respectively, were not evaluable. No objective responses occurred in either BID or TID dose escalation cohorts. Best response of stable disease (SD) occurred in 7/27 (25.9%) patients in TID and 10/16 (62.5%) patients in BID dose escalation. In dose expansion, 1/58 patients had a PR (in an RCC patient), 24/58 (41.4%) had SD, 33/58 (56.9%) had PD (**Table 4**). SDs occurred across different tumor types, with time on study extending to ≥6 months for 12 patients (**Fig. 2A** and **B**).

Patients with RCC exhibited more prominent clinical activity than other tumor types and were prioritized for further study. One of 9 RCC dose-expansion patients attained a PR, prompting expansion of the RCC cohort. Patient characteristics from the RCC expansion cohort ($n = 22$) were similar to the overall population (median age 65 years, 45% female, heavily pretreated; 65% with >3 prior systemic therapies). Data were not evaluable for 1 and 2 patients with RCC in dose escalation and dose expansion, respectively. Among 28 evaluable patients with RCC in both dose escalation and dose expansion, DCR was 14/28 (50%; **Table 4**).

The patients with RCC who achieved a PR had been diagnosed with metastatic clear cell RCC, receiving 3 prior lines of systemic therapy (sunitinib, pazopanib, everolimus; immediate prior treatment duration: 4.6 months; best response: PD). Treatment with telaglenastat led to a 32% reduction in target lesions and complete resolution of lymphadenopathy, whereas an adrenal target lesion remained unchanged (**Fig. 2C**). Duration of response was 7.4 months. PK data from the patient showed high telaglenastat exposure (AUC: 19,900 ng•hr/mL, C_{max} 2,960 ng/mL; C_{min} 1,490 ng/mL). Four patients with RCC remained on study for more than 10 months, including one clear cell patient with RCC who remained on for >2.4 years.

Table 3. Pharmacokinetics of telaglenastat.

	Steady-state plasma exposure on C1D15 by dose level, mean (CV%)								
	TID-fasted						BID-fed		
PK Parameter	100 mg ($n = 2$)	150 mg ($n = 4$)	250 mg ($n = 7$)	400 mg ($n = 3$)	600 mg ($n = 5$)	800 mg ($n = 3$)	600 mg ($n = 41$)	800 mg ($n = 10$)	1,000 mg ($n = 4$)
AUC_{0-8h} ng·h/mL	2,150 (57.2)	7,603 (100.7)	4,626 (96.5)	3,850 (33.5)	5,162 (75.3)	5,832 (73.5)	7,611 (65.4)	9,660 (56.7)	5,073 (118.8)
C_{min}, ng/mL[a]	147 (89.0–204)	355 (131–1,830)	126 (51–753)	186 (171–536)	231 (19–471)	232 (205–878)	348 (262–1,030)	443 (374–1,090)	147 (73.2–221)
C_{max}, ng/mL	395 (66.9)	1,444 (83.2)	914 (90.0)	818 (17.6)	1,142 (75.5)	1,058 (34.5)	1,455 (54.1)	1,774 (60.5)	915 (121.5)
t_{max}, h (range)	1.54 (1.08–2.00)	1.00 (0.50–3.98)	2.00 (0.50–7.83)	1.00 (0.25–7.83)	1.03 (0.50–4.00)	2.02 (1.00–7.83)	4.00 (0.48–8.08)	4.00 (1.98–6.15)	6.08 (5.98–6.17)
Intrapatient ratios following administration of TID telaglenastat under fed (C2D1) vs. fasted (C1D15) conditions, mean (CV%)[b]									
	100 mg ($n = 1$)	150 mg ($n = 4$)	250 mg ($n = 4$)	400 mg ($n = 2$)	600 mg ($n = 2$)	800 mg ($n = 3$)	All doses combined (100–800 mg) $N = 16$		
$AUC_{0-8h\ C2D1}/AUC_{0-8h\ C1D15}$	1.26 (NC)	1.60 (62.0)	1.46 (20.6)	1.83 (69.4)	1.36 (83.3)	1.56 (38.2)	1.53 (45.0)		
$C_{max\ C2D1}/C_{max\ C1D15}$	1.20 (NC)	1.28 (49.5)	1.40 (17.6)	1.89 (41.1)	1.56 (66.1)	1.86 (44.3)	1.52 (39.4)		
$t_{max\ C2D1}/t_{max\ C1D15}$	3.72 (NC)	5.83 (51.8)	1.50 (82.0)	12.1 (135.6)	10.5 (70.5)	2.21 (148.4)	5.30 (120.5)		

Abbreviations: AUC_{0-8h}, area under the plasma drug concentration-time curve from time zero to the last measurable concentration; BID, twice daily; C1D15, cycle 1 day 15; C2D1, cycle 2 day 1; C_{max}, maximum observed plasma concentration; C_{min}, minimum observed plasma concentration; CV%, coefficient of variation; NC, not calculated; PK, pharmacokinetic; TID, 3 times daily; t_{max}, time of maximum observed plasma concentration.

[a]Median (range).

[b]Data from patients treated with proton pump inhibitors were excluded.

Discussion

In this first-in-human study, we sought to define the safety profile and RP2D of telaglenastat in patients with advanced, treatment-refractory solid tumors. Telaglenastat was well tolerated at all evaluated dose levels. MTD was not reached. Based upon composite review of the safety profile, PK profile, and pharmacodynamic effect (i.e., GLS inhibition in platelets and tumors), the RP2D was set at 800 mg BID-fed.

The delayed absorption and flattened PK profile, together with the favorable PK/PD profile demonstrating efficient GLS inhibition and the safety profile under BID-fed conditions, supported the selection of the BID-fed dosing regimen. For all patients at higher dose levels (600–800 mg BID-fed), mean pre-dose plasma telaglenastat concentrations on day 15 of cycle 1 or day 1 of cycle 2, met or exceeded the 250 ng/mL level required for saturating GLS inhibition at >95% in platelets. Exposure to telaglenastat following single or multiple administrations was higher under fed conditions than fasted, supporting BID-fed dosing for telaglenastat. Although interpatient variability was high, exposure did generally increase with dose in a less than dose proportional manner. Pharmacodynamic assessment indicated that telaglenastat inhibited GLS activity in both platelets and tumors, and, consistent with its mechanism-of-action, plasma glutamine levels rose in patients approximately 1.5-fold on average.

In preclinical studies, GLS inhibition has not shown toxic effects in noncancerous cells (Calithera, data on file). However, given the importance of glutamine for normal cell metabolism, it was important to establish the safety profile of telaglenastat in this study. Telaglenastat was well tolerated, with a low rate of grade 3/4 treatment-related AEs, particularly in the BID dose cohorts. The most common treatment-related AEs of any grade were fatigue (23%), nausea (19%), ALT increased (17%), AST increased (13%), and photophobia (11%). Hepatic AEs were strictly laboratory abnormalities, typically AST and/or ALT elevations that were transient and reversible. There were no cases of drug-induced liver injury according to the Hy's law criteria. Importantly, the proportion of treatment-related grade ≥3 events was markedly lower on the BID-fed schedule compared with the TID-fasted schedule (3% vs. 22%). Notably, grade 3 AST/ALT increase was reduced to 1%–2% on the BID-fed schedule with no grade 4 elevations.

Exploration of antitumor activity in expansion cohorts in tumor types associated with glutamine dependency in the literature showed modest single-agent antitumor activity of primarily in the form of stable disease. In patients with late-line treatment-refractory RCC, one confirmed PR occurred in a patient who remained on study for approximately 12 months, and the overall DCR was 50%. Although these observations might be attributed to disease favorable disease biology, our findings may also reflect clinical cytostatic activity of GLS inhibition, which was observed in the preclinical *in vivo* models of telaglenastat in RCC as well as in the clinical with other agents that interfere with tumor metabolism in solid tumors (i.e., IDH inhibitors; ref. 34).

Limitations of this study for evaluating efficacy include small cohorts, lack of an active control, and the dose-escalation design leading to many patients being treated below the RP2D. In particular, NSCLC, *MYC* amplification, mesothelioma, and the individual TCA mutant tumor cohorts had small sample sizes limiting efficacy assessments. PK/PD analyses were also limited by the different time points used for data collection, the small number of tumor samples available for correlative studies (which led to the use of platelets as a surrogate), and general challenges with biomarker studies in patient tumor tissues.

Published OnlineFirst July 20, 2021; DOI: 10.1158/1078-0432.CCR-21-1204

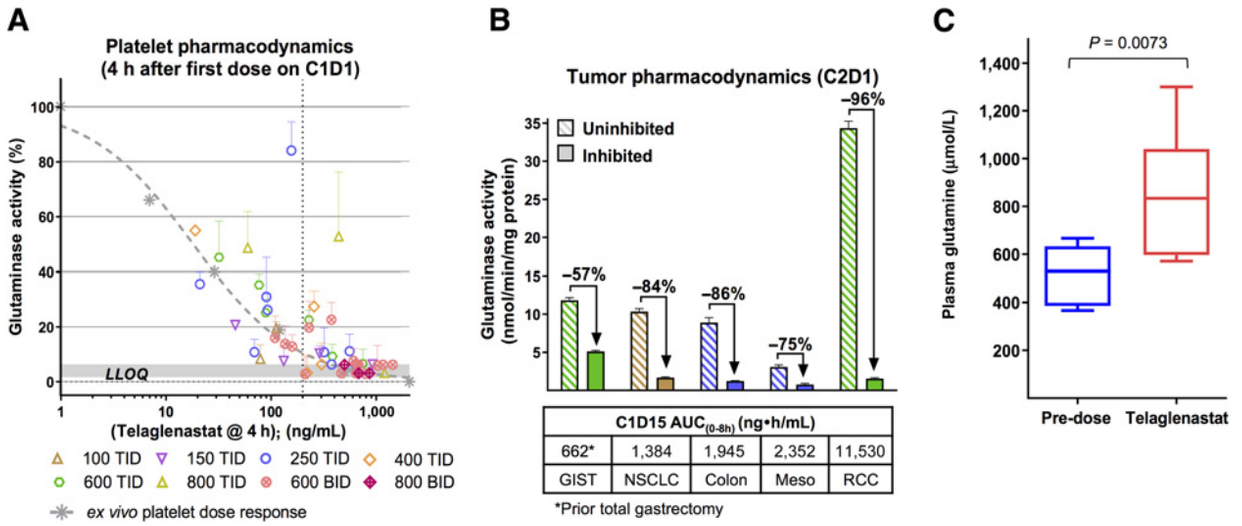

Figure 1.

Telaglenastat pharmacodynamics. **A,** GLS activity in platelets isolated from blood collected 4 hours after the first dose of telaglenastat on cycle 1 day 1. GLS activity was measured with a coupled enzymatic assay, and the percent GLS inhibition was determined by comparison with predose samples. **B,** GLS activity in fresh tumor biopsies collected on cycle 2 day 1. GLS activity was determined under assay conditions that preserve the telaglenastat/GLS complex (inhibited activity) or allow telaglenastat to fully dissociate from GLS (uninhibited activity). The first pair of samples showing 57% GLS inhibition was from a patient who had low systemic exposure, likely due to radical gastrectomy. **C,** Increase in plasma glutamine concentration from predose to cycle 1 day 15 post-telaglenastat dosing ($n = 6$). AUC, area under the curve; BID, twice daily; C, cycle; D, day; GIST, gastrointestinal stromal tumor; NSCLC, non–small cell lung cancer; meso, mesothelioma; RCC, renal cell carcinoma; TID, three times daily.

Since the conception of this study, additional evidence has emerged suggesting that GLS inhibition and/or glutamine depletion alone may not be sufficient in an unselected patient population and emerging data indicate that rational combination of telaglenastat with other therapies and in biomarker-selected patient populations may be required to enhance antitumor efficacy (35). To this aim, telaglenastat has been explored in combination with everolimus or cabozantinib, agents known to interfere with glucose utilization. Dual inhibition of glucose and glutamine metabolism in preclinical models augments anticancer activity over monotherapy and a recent phase Ib study of telaglenastat plus everolimus or cabozantinib in treatment refractory RCC exhibited favorable results. Data from these studies prompted two proof-of-concept, phase II randomized trials, ENTRATA (NCT03163667), and CANTATA (NCT03428217), evaluating the addition telaglenastat to cabozantinib in patient with RCC (36, 37). Results from these studies will be described separately. Several other clinical studies will clarify the role of glutamine depletion in advanced solid tumors, including the phase II KEAPSAKE trial in NSCLC (NCT04265534). KEAPSAKE is evaluating telaglenastat in combination with standard-of-care therapy in patients with NSCLC who harbor *KEAP1/NRF2* mutations that drive glutamine metabolism and glutathione generation as a means to cancer cell protection from proliferative and treatment-induced oxidative stress (38).

In summary, this first-in-human phase I study established an RP2D for telaglenastat in patients with solid tumors, revealed favorable PK/PD and safety profiles, demonstrated robust target GLS inhibition, and showed early signals of anticancer activity that warrant further exploration. Future and ongoing studies seek to explore how we can use biomarker selection, such as *KEAP1/NRF2* mutations in NSCLC, or with novel combinations, including immuno-oncology therapies, and with mTOR inhibition.

Table 4. Summary of best overall response rates in efficacy evaluable patients.

	Dose escalation			RCC cohorts		
	TID-fasted ($N = 27$)	BID-fed ($N = 16$)	All dose expansion ($N = 58$)	Dose escalation ($n = 8$)	Dose expansion ($n = 20$)	All RCC ($n = 28$)
Partial response	0	0	1 (1.7)	0	1 (5.0)	1 (3.6)
Stable disease	7 (25.9)	10 (62.5)	24 (41.4)	5 (62.5)	8 (40.0)	13 (46.4)
Progressive disease	20 (74.1)	6 (37.5)	33 (56.9)	3 (37.5)	11 (55.0)	14 (50.0)
Disease control rate[a]	7 (25.9)	10 (62.5)	25 (43.1)	5 (62.5)	9 (45.0)	14 (50.0)

Note: The efficacy analysis set comprised all patients who completed one post-baseline tumor assessment; patients who discontinued study medication early due to study drug–related toxicity or due to disease-related death or symptomatic deterioration (clinical progression) and had received at least 48 doses TID or 32 doses BID were considered evaluable for efficacy.

Abbreviations: BID, twice daily; RCC, renal cell carcinoma; TID, three times daily.

[a]DCR, overall response rate + stable disease.

Published OnlineFirst July 20, 2021; DOI: 10.1158/1078-0432.CCR-21-1204

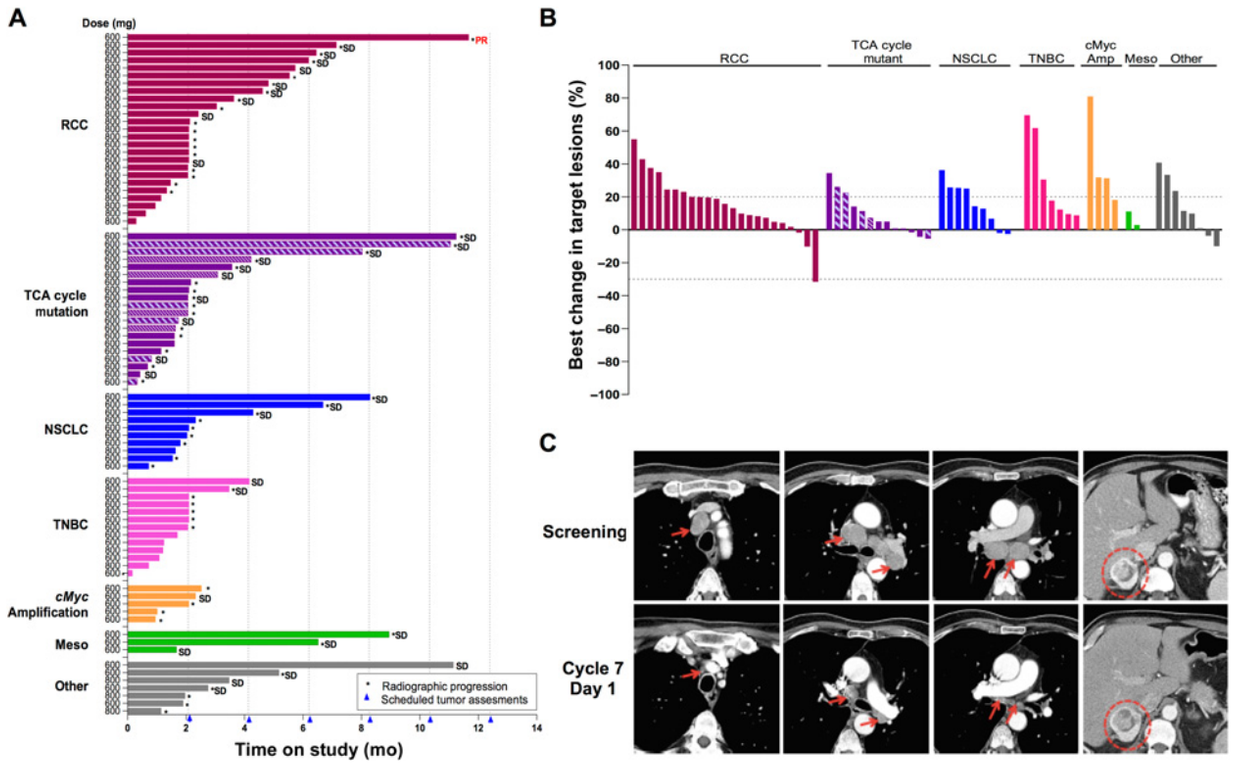

Figure 2.

Telaglenastat activity. **A,** Time on study for patients receiving telaglenastat 600 or 800 mg BID. **B,** Best change in target lesions in efficacy evaluable patients receiving telaglenastat 600 or 800 mg BID. **C,** Computed tomography (CT) scans taken on cycle 1 day 15 from clear cell RCC (800 mg BID) with partial response. meso, mesothelioma; NSCLC, non–small cell lung cancer; RCC, renal cell carcinoma; TCA, citric acid cycle; TNBC, triple-negative breast cancer. For TCA cycle mutations, patients with IDH mutations are represented by solid bars, SDH mutations by thick hatched bars, and FH mutations by thin hatched bars.

Authors' Disclosures

J.J. Harding reports grants from Bristol Myers Squibb and personal fees from Bristol Myers Squibb, Merck, Eisai, Exelexis, Eli Lilly, Imvax, CytomX, Adaptimmune, QED, and Zymeworks outside the submitted work. M. Telli reports grants from Calithera, Tesaro, Biothera, Vertex, EMD Serono, and Bayer during the conduct of the study, as well as personal fees from Celldex, Immunomedics, Daiichi Sankyo, Lilly, Celgene, Natera, Blueprint Medicines, G1 Therapeutics, and AstraZeneca, and grants and personal fees from Genentech, Merck, AbbVie, Pfizer, and OncoSec Medical outside the submitted work. P. Munster reports grants from UCSF during the conduct of the study. M.H. Voss reports grants and personal fees from Pfizer, as well as personal fees from Eisai, Chengdu, Exelixis, Corvus, Merck, and Aveo outside the submitted work. J.R. Infante reports grants from Calithera Therapeutics during the conduct of the study, as well as personal fees from Janssen Pharmaceuticals outside the submitted work. A. DeMichele reports grants from Pfizer, Novartis, Calithera, and Genetech outside the submitted work. M. Dunphy reports grants from National Institutes of Health during the conduct of the study. M.H. Le reports other support from Calithera Biosciences, Inc. during the conduct of the study; other support from Calithera Biosciences, Inc. outside the submitted work; and a patent for Methods of Administering Glutaminase Inhibitors pending. C. Molineaux reports other support from Calithera Biosciences during the conduct of the study; other support from Calithera Biosciences outside the submitted work; and a patent for Calithera Biosciences pending to Calithera Biosciences. K. Orford reports personal fees from Calithera Biosciences during the conduct of the study; personal fees from Calithera Biosciences outside the submitted work; and equity in Calithera Biosciences. N.M. Tannir reports grants and personal fees from Calithera Bioscience, Bristol-Myers Squibb, Pfizer, Nektar Therapeutics, and Exelisis, Inc., during the conduct of the study, as well as personal fees from Eisai Medical Research, Lilly, and Oncorena outside the submitted work. F. Meric-Bernstam reports grants from Calithera Biosciences, Aileron Therapeutics, Inc., AstraZeneca, Bayer Healthcare Pharmaceutical, Curis Inc., CytomX Therapeutics Inc., Daiichi Sankyo Co. Ltd., Debiopharm International, eFFECTOR Therapeutics, Genentech Inc., Guardant Health Inc., Klus Pharma, Takeda Pharmaceutical (formerly Millennium Pharmaceutical), Novartis, Puma Biotechnology Inc., and Taiho Pharmaceutical Co. during the conduct of the study, as well as personal fees from AbbVie, Aduro BioTech Inc., Alkermes, AstraZeneca, DebioPharm, eFFECTOR Therapeutics, F. Hoffman-La Roche Ltd., Genentech Inc., IBM Watson, Infinity Pharmaceuticals, The Jackson Laboratory, Kolon Life Science, OrigiMed, PACT Pharma, Parexel International, Pfizer Inc., Samsung Bioepis, Seattle Genetics Inc., Tyra Biosciences, Xencor, Zymeworks, Black Diamond, Eisai, Immunomedics, Inflection Biosciences, Karyopharm Therapeutics, Mersana Therapeutics, OnCusp Therapeutics, Puma Biotechnology Inc., Seattle Genetics, Silverback Therapeutics, Spectrum Pharmaceuticals, Zentalis, Chugai Biopharmaceuticals, Mayo Clinic, and Rutgers Cancer Institute of New Jersey outside the submitted work. No disclosures were reported by the other authors.

Authors' Contributions

J.J. Harding: Investigation, writing–original draft, writing–review and editing. **M. Telli:** Investigation, writing–review and editing. **P. Munster:** Investigation, writing–review and editing. **M.H. Voss:** Investigation, writing–review and editing. **J.R. Infante:** Investigation, writing–review and editing. **A. DeMichele:** Investigation, writing–review and editing. **M. Dunphy:** Investigation, writing–review and editing. **M.H. Le:** Conceptualization, formal analysis, methodology, writing–review and editing. **C. Molineaux:** Conceptualization, formal analysis, methodology, writing–review and editing. **K. Orford:** Conceptualization, formal analysis, methodology, writing–review and editing. **F. Parlati:** Conceptualization, writing–review and editing. **S.H. Whiting:** Conceptualization, formal analysis, methodology, writing–review and editing. **M.K. Bennett:** Conceptualization, formal analysis, methodology,

authorship is posthumous and based on his contribution before his passing. **N.M. Tannir:** Investigation, writing–review and editing. **F. Meric-Bernstam:** Investigation, writing–review and editing.

Acknowledgments

We thank the investigators and site staff and patients and their families for their participation in the study. Editorial support was provided by Ingrid Koo, PhD, and funded by Calithera Biosciences, Inc.

The costs of publication of this article were defrayed in part by the payment of page charges. This article must therefore be hereby marked *advertisement* in accordance with 18 U.S.C. Section 1734 solely to indicate this fact.

Received March 31, 2021; revised June 2, 2021; accepted July 15, 2021; published first July 20, 2021.

References

1. Hensley CT, Wasti AT, DeBerardinis RJ. Glutamine and cancer: cell biology, physiology, and clinical opportunities. J Clin Invest 2013;123:3678–84.
2. Altman BJ, Stine ZE, Dang CV. From Krebs to clinic: glutamine metabolism to cancer therapy. Nat Rev Cancer 2016;16:749.
3. DeBerardinis RJ, Mancuso A, Daikhin E, Nissim I, Yudkoff M, Wehrli S, et al. Beyond aerobic glycolysis: transformed cells can engage in glutamine metabolism that exceeds the requirement for protein and nucleotide synthesis. Proc Natl Acad Sci U S A 2007;104:19345–50.
4. Parlati F, Demo SD, Gross MI, Janes JR, Lewis ER, Mackinnon AL, et al. CB-839, a novel potent and selective glutaminase inhibitor, has broad antiproliferative activity in cell lines derived from both solid tumors and hematological malignancies [abstract]. In: Proceedings of the 105th Annual Meeting of the American Association for Cancer Research; 2014 Apr 5-9; San Diego, CA. Philadelphia (PA): AACR; 2014. p. 74. Abstract nr 1416.
5. Cassago A, Ferreira AP, Ferreira IM, Fornezari C, Gomes ER, Greene KS, et al. Mitochondrial localization and structure-based phosphate activation mechanism of Glutaminase C with implications for cancer metabolism. Proc Natl Acad Sci U S A 2012;109:1092–7.
6. Kung HN, Marks JR, Chi JT. Glutamine synthetase is a genetic determinant of cell type-specific glutamine independence in breast epithelia. PLoS Genet 2011;7:e1002229.
7. Le A, Lane AN, Hamaker M, Bose S, Gouw A, Barbi J, et al. Glucose-independent glutamine metabolism via TCA cycling for proliferation and survival in B cells. Cell Metab 2012;15:110–21.
8. Seltzer MJ, Bennett BD, Joshi AD, Gao P, Thomas AG, Ferraris DV, et al. Inhibition of glutaminase preferentially slows growth of glioma cells with mutant IDH1. Cancer Res 2010;70:8981–7.
9. Son J, Lyssiotis CA, Ying H, Wang X, Hua S, Ligorio M, et al. Glutamine supports pancreatic cancer growth through a KRAS-regulated metabolic pathway. Nature 2013;496:101–5.
10. van den Heuvel AP, Jing J, Wooster RF, Bachman KE. Analysis of glutamine dependency in non-small cell lung cancer: GLS1 splice variant GAC is essential for cancer cell growth. Cancer Biol Ther 2012;13:1185–94.
11. Wang JB, Erickson JW, Fuji R, Ramachandran S, Gao P, Dinavahi R, et al. Targeting mitochondrial glutaminase activity inhibits oncogenic transformation. Cancer Cell 2010;18:207–19.
12. Gameiro PA, Yang J, Metelo AM, Perez-Carro R, Baker R, Wang Z, et al. In vivo HIF-mediated reductive carboxylation is regulated by citrate levels and sensitizes VHL-deficient cells to glutamine deprivation. Cell Metab 2013;17:372–85.
13. Okazaki A, Gameiro PA, Christodoulou D, Laviollette L, Schneider M, Chaves F, et al. Glutaminase and poly(ADP-ribose) polymerase inhibitors suppress pyrimidine synthesis and VHL-deficient renal cancers. J Clin Invest 2017;127:1631–45.
14. Commisso C, Davidson SM, Soydaner-Azeloglu RG, Parker SJ, Kamphorst JJ, Hackett S, et al. Macropinocytosis of protein is an amino acid supply route in Ras-transformed cells. Nature 2013;497:633–7.
15. Alles MC, Gardiner-Garden M, Nott DJ, Wang Y, Foekens JA, Sutherland RL, et al. Meta-analysis and gene set enrichment relative to er status reveal elevated activity of MYC and E2F in the "basal" breast cancer subgroup. PLoS ONE 2009;4:e4710.
16. Chandriani S, Frengen E, Cowling VH, Pendergrass SA, Perou CM, Whitfield ML, et al. A core MYC gene expression signature is prominent in basal-like breast cancer but only partially overlaps the core serum response. PLoS ONE 2009;4:e6693.
17. Gatza ML, Lucas JE, Barry WT, Kim JW, Wang Q, Crawford MD, et al. A pathway-based classification of human breast cancer. Proc Natl Acad Sci U S A 2010;107:6994–9.
18. Gao P, Tchernyshyov I, Chang TC, Lee YS, Kita K, Ochi T, et al. c-Myc suppression of miR-23a/b enhances mitochondrial glutaminase expression and glutamine metabolism. Nature 2009;458:762–5.
19. Yuneva MO, Fan TW, Allen TD, Higashi RM, Ferraris DV, Tsukamoto T, et al. The metabolic profile of tumors depends on both the responsible genetic lesion and tissue type. Cell Metab 2012;15:157–70.
20. Collins RRJ, Patel K, Putnam WC, Kapur P, Rakheja D. Oncometabolites: a new paradigm for oncology, metabolism, and the clinical laboratory. Clin Chem 2017;63:1812–20.
21. Mullen AR, Wheaton WW, Jin ES, Chen PH, Sullivan LB, Cheng T, et al. Reductive carboxylation supports growth in tumour cells with defective mitochondria. Nature 2011;481:385–8.
22. McBrayer SK, Mayers JR, DiNatale GJ, Shi DD, Khanal J, Chakraborty AA, et al. Transaminase Inhibition by 2-hydroxyglutarate impairs glutamate biosynthesis and redox homeostasis in glioma. Cell 2018;175:101–16.
23. Gross MI, Demo SD, Dennison JB, Chen L, Chernov-Rogan T, Goyal B, et al. Antitumor activity of the glutaminase inhibitor CB-839 in triple-negative breast cancer. Mol Cancer Ther 2014;13:890–901.
24. Rodriguez ML, Zhang W, Bennett MK, Emberley E, Gross MI, Janes JR, et al. CB-839, a selective glutaminase inhibitor, synergizes with signal transduction pathway inhibitors to enhance antitumor activity. Cancer Res 2015;75:15.
25. Parlati F, Bromley-Dulfano S, Demo SD, Janes JR, Gross MI, Lewis ER, et al. Antitumor activity of the glutaminase inhibitor CB-839 in hematological malignances. Blood 2013;122:4226.
26. Emberley E, Bennett MK, Chen J, Gross MI, Huang T, Li W, et al. CB-839, a selective glutaminase inhibitor, has antitumor activity in renal cell carcinoma and synergizes with everolimus and receptor tyrosine kinase inhibitors. Eur J Cancer 2016;69:S124.
27. Mackinnon AL, Chen J, Gross MI, Marguier G, Shwonek PJ, Sotirovska N, et al. Targeting tumor glutamine metabolism with CB-839 enhances the efficacy of immune checkpoint inhibitors. J Immunother Cancer 2016;4:P224.
28. Parlati F, Chernov-Rogan T, Demo SD, Gross MI, Janes JR, Kawas R, et al. Antitumor activity of novel, potent, selective, and orally-bioavailable glutaminase inhibitors. Cancer Res 2013;73:8.
29. Parlati F, Gross MI, Janes JR, Lewis ER, Mackinnon AL, Rodriguez ML, et al. Glutaminase inhibitor CB-839 synergizes with pomalidomide in preclinical multiple myeloma models. Blood 2014;124:4720.
30. Thompson RM, Dytfeld D, Reyes L, Robinson RM, Smith B, Manevich Y, et al. Glutaminase inhibitor CB-839 synergizes with carfilzomib in resistant multiple myeloma cells. Oncotarget 2017;8:35863–76.
31. Lampa M, Arlt H, He T, Ospina B, Reeves J, Zhang B, et al. Glutaminase is essential for the growth of triple-negative breast cancer cells with a deregulated glutamine metabolism pathway and its suppression synergizes with mTOR inhibition. PLoS ONE 2017;12:e0185092.
32. Eisenhauer EA, Therasse P, Bogaerts J, Schwartz LH, Sargent D, Ford R, et al. New response evaluation criteria in solid tumours: revised RECIST guideline (version 1.1). Eur J Cancer 2009;45:228–47.
33. Byrne MJ, Nowak AK. Modified RECIST criteria for assessment of response in malignant pleural mesothelioma. Ann Oncol 2004;15:257–60.
34. Lowery MA, Burris HA III, Janku F, Shroff RT, Cleary JM, Azad NS, et al. Safety and activity of ivosidenib in patients with IDH1-mutant advanced cholangiocarcinoma: a phase 1 study. Lancet Gastroenterol Hepatol 2019;4:711–20.
35. Romero R, Sayin VI, Davidson SM, Bauer MR, Singh SX, LeBoeuf SE, et al. Keap1 loss promotes Kras-driven lung cancer and results in dependence on glutaminolysis. Nat Med 2017;23:1362–8.

36. Motzer R, Lee C-H, Emamekhoo H, Matrana M, Percent I, Hsieh J, et al. ENTRATA: randomized, double-blind, phase 2 study of telaglenastat (tela; CB-839) + everolimus (E) vs. placebo (pbo) + E in patients (pts) with advanced/metastatic renal cell carcinoma (mRCC). Ann Oncol 2019;30: v851–934.
37. Tannir N, Agarwal N, Porta C, Lawrence N, Motzer R, Lee R, et al. CANTATA: Primary analysis of a global, randomized, placebo (Pbo)-controlled, double-blind trial of telaglenastat (CB-839) + cabozantinib vs. Pbo + cabozantinib in patients (pts) with advanced/metastatic renal cell carcinoma (mRCC) that progressed on immune checkpoint inhibitor (ICI) or anti-angiogenic therapies. J Clin Oncol 2021;39:15.
38. ClinicalTrials.gov. KEAPSAKE: a study of Telaglenastat (CB-839) with standard-of-care chemoimmunotherapy in 1L KEAP1/NRF2-mutated, nonsquamous NSCLC (KEAPSAKE). Bethesda (MD): National Library of Medicine. Available from: <https://clinicaltrials.gov/ct2/show/NCT04265534>.

AACR American Association for Cancer Research

Clinical Cancer Research

A Phase I Dose-Escalation and Expansion Study of Telaglenastat in Patients with Advanced or Metastatic Solid Tumors

James J. Harding, Melinda Telli, Pamela Munster, et al.

Clin Cancer Res 2021;27:4994-5003. Published OnlineFirst July 20, 2021.